In vivo engineering of bone tissues with hematopoietic functions and mixed chimerism

Yu-Ru Shih[a], Heemin Kang[a,b], Vikram Rao[a], Yu-Jui Chiu[b], Seong Keun Kwon[a,c], and Shyni Varghese[a,b,1]

[a]Department of Bioengineering, University of California, San Diego, La Jolla, CA 92093; [b]Materials Science and Engineering Program, University of California, San Diego, La Jolla, CA 92093; and [c]Department of Otorhinolaryngology—Head and Neck Surgery, Seoul National University Hospital, Seoul 110-774, Republic of Korea

Edited by Robert Langer, MIT, Cambridge, MA, and approved April 17, 2017 (received for review February 15, 2017)

Synthetic biomimetic matrices with osteoconductivity and osteoinductivity have been developed to regenerate bone tissues. However, whether such systems harbor donor marrow in vivo and support mixed chimerism remains unknown. We devised a strategy to engineer bone tissues with a functional bone marrow (BM) compartment in vivo by using a synthetic biomaterial with spatially differing cues. Specifically, we have developed a synthetic matrix recapitulating the dual-compartment structures by modular assembly of mineralized and nonmineralized macroporous structures. Our results show that these matrices incorporated with BM cells or BM flush transplanted into recipient mice matured into functional bone displaying the cardinal features of both skeletal and hematopoietic compartments similar to native bone tissue. The hematopoietic function of bone tissues was demonstrated by its support for a higher percentage of mixed chimerism compared with i.v. injection and donor hematopoietic cell mobilization in the circulation of nonirradiated recipients. Furthermore, hematopoietic cells sorted from the engineered bone tissues reconstituted the hematopoietic system when transplanted into lethally irradiated secondary recipients. Such engineered bone tissues could potentially be used as ectopic BM surrogates for treatment of nonmalignant BM diseases and as a tool to study hematopoiesis, donor–host cell dynamics, tumor tropism, and hematopoietic cell transplantation.

tissue engineering | regenerative medicine | mixed chimerism | stem cells | bone marrow

Transplantation of hematopoietic stem cells (HSCs) or bone marrow (BM) cells is increasingly being used as a standard care of treatment for diverse life-threatening blood disorders, including hematologic malignancies, immune system disorders, metabolic diseases, hemoglobinopathies, and auto-immune diseases (1–6). Successful allogeneic HSC or BM transplantation relies heavily on the ability of the HLA-matched donor cells to replace the recipient's hematopoietic functions by homing and engrafting into the host BM niche (7–9). Currently, all transplantations require recipient conditioning, which involves cytoreductive agents and/or irradiation to improve donor cell engraftment (10–12). The conditioning provides immunosuppression and allows for donor cells to engraft in the recipient HSC niche (12, 13). However, such conditioning regimens are often accompanied by short-term and long-term adverse effects in patients (12, 14–16). An extramedullary marrow that acts as a reservoir for donor BM cells by contributing to adequate mixed chimerism, without the need for recipient conditioning, would potentially benefit patients by reducing side effects and the donor cell numbers needed with curative outcomes.

Several studies have shown host-cell–mediated hematopoiesis in ectopic bone tissues (17–25). These approaches include implantation of osteoinductive materials like demineralized bone powder (20), bone shafts (18), cell-laden synthetic or biological biomaterials (19, 21–26) in ectopic sites such as s.c. tissue, small bowel mesentery, or subrenal capsule. These studies have demonstrated that engineered ectopic bone tissues can recruit host hematopoietic cells (17–22, 26) or attract i.v.-administered donor hematopoietic progenitor cells to reconstitute the BM environment (23–25, 27).

HSCs reside in BM in close proximity with calcified endosteal bone and the perivascular niche; the cellular and noncellular components of the niche play a key role in hematopoiesis (28–37). Leveraging these understandings, we hypothesize that osteoinductive synthetic scaffolds loaded with hematopoietic cells could result in ectopic bone tissues with hematopoiesis in a spatially confined manner similar to native long-bone tissue. We explored the potential of tissue-engineered ectopic bone tissues with a marrow compartment as a reservoir for donor BM cells and the ability of such a system to establish mixed chimerism in the recipient. To this end, we have developed a biomaterial displaying a dual-compartment structure with an outer osteoinductive mineralized shell encasing either a nonmineralized macroporous inner layer or a hollow core for loading with bone marrow cells (BMC) or bone marrow flush (BMF), respectively. Our findings demonstrate that the outer shell of the implants matured into calcified bone in vivo with an inner hematopoietic compartment that supports long-term hematopoietic maintenance. Furthermore, the donor hematopoietic cells within the engineered bone yielded a higher mixed chimerism in the circulation of recipient mice compared with that of i.v. injections and responded to a hematopoietic stem cell mobilization agent.

Results and Discussion

Development of Monolithic and Dual-Compartment Matrices. Macroporous matrices with interconnected pores were fabricated by poly(methyl methacrylate) templating of poly(ethylene glycol)-diacrylate-*co*-*N*-acryloyl 6-aminocaproic acid (A6ACA) (PEGDA-*co*-A6ACA) (*SI Appendix*, Fig. S1 and *SI Experimental Procedures*).

Significance

Current bone marrow (BM) or hematopoietic stem cell (HSC) transplantations require recipient conditioning that is accompanied by significant adverse effects in patients. Here, we report engineering of bone tissues with a functional BM compartment in vivo by modular assembly of mineralized and nonmineralized macroporous structures. These engineered bone tissues support maintenance of donor hematopoietic cells, respond to an HSC mobilization agent, and yield higher mixed chimerism in circulation of nonirradiated recipient mice compared with that of intravenous transplantation. Such engineered bone tissues could potentially be used as ectopic BM surrogates to treat various nonmalignant BM diseases and as a tool to study hematopoiesis, donor–host cell dynamics, tumor tropism, and hematopoietic cell transplantation.

Author contributions: Y.-R.S. and S.V. designed research; Y.-R.S., H.K., V.R., Y.-J.C., and S.K.K. performed research; Y.-R.S., H.K., and S.V. analyzed data; and Y.-R.S., H.K., and S.V. wrote the paper.

The authors declare no conflict of interest.

This article is a PNAS Direct Submission.

[1]To whom correspondence should be addressed. Email: svarghese@ucsd.edu.

This article contains supporting information online at www.pnas.org/lookup/suppl/doi:10.1073/pnas.1702576114/-/DCSupplemental.

Details of the synthesis of precursors as well as formation of macroporous matrices and their mineralization are described elsewhere (38–41). The nonmineralized and mineralized matrices were assembled to create a dual-compartment structure with the outer compartment mineralized and the inner compartment either nonmineralized or hollow, emulating the structure of long-bone tissue (*SI Appendix*, Figs. S1 and S2*A* and *SI Experimental Procedures*). In the case of dual-compartment matrices with a nonmineralized macroporous inner compartment, structures with two different inner dimensions (4-mm length × 1.5-mm radius vs. 1-mm length × 0.5-mm radius) were prepared. Characterization of the matrices by scanning electron microscopy (SEM) showed an interconnected porous network with a plate-like morphology of matrix-bound calcium phosphate (CaP) minerals that were confined within the mineralized compartment with no such minerals detected in the inner compartment (*SI Appendix*, Fig. S2*A*). The presence of CaP minerals in the outer compartment was further identified by elemental analysis that revealed a calcium/phosphorus (Ca/P) ratio of 1.38. As determined from the SEM images, the nonmineralized and mineralized macroporous compartments exhibited a pore diameter of 104.6 μm ± 18.9 μm and 82.2 μm ± 15.3 μm in their dried state, respectively (*SI Appendix*, Fig. S2*B*). The pore sizes of the macroporous mineralized and nonmineralized structures were found to be 112.7 μm ± 6.9 μm and 111.1 μm ± 6.8 μm, respectively, in their swollen state (*SI Appendix*, Fig. S2*C*).

Nonmineralized and Mineralized Matrices in the Function of Bone-Marrow–Derived Cells. The effects of nonmineralized and mineralized matrices on promoting osteogenic differentiation of mesenchymal stromal cells and maintenance of hematopoietic cells were determined by using monolithic matrices. Consistent with our prior studies involving human stem cells (42–44), the mouse mesenchymal stromal cells (mMSCs) cultured within the mineralized matrices underwent osteogenic differentiation in vitro in growth medium lacking any osteogenic-inducing molecules (*SI Appendix*, Fig. S3 *A* and *B*). No such osteogenic differentiation was observed for mMSCs cultured on corresponding nonmineralized matrices. By contrast, the nonmineralized matrices consistently maintained a higher percentage of human CD34-positive cells than mineralized matrices after 14 d of in vitro culture (*SI Appendix*, Fig. S4 *A* and *B*). In vivo implantation of BMC-loaded monolithic matrices showed significantly higher numbers of long term-HSCs (LT-HSCs) in nonmineralized matrices compared with mineralized matrices (*SI Appendix*, Fig. S4*C*). However, this in vivo finding should be considered noting that the implanted BMC-laden nonmineralized matrices undergo auto-calcification in vivo (calcification observed mainly along the periphery of the implant) mostly due to the presence of 6-aminocaproic acid (A6ACA) moieties that can facilitate mineralization by binding to $Ca2^{+}$ in the milieu. Previously, we have shown that human embryonic stem cell-loaded nonmineralized PEGDA-*co*-A6ACA scaffolds in vivo progressed to form spatially distinct bone and fat tissues with calcification and bone tissue formation confined mostly along the periphery (43).

Spatially Controlled Formation of Bone Tissue Harboring Donor Hematopoietic Cells. The dual-compartment matrices were seeded with either BMC or BMF at an initial total cell number of ~5.2×10^7 cells (corresponding to ~5×10^7 CD45-positive hematopoietic cells). In the case of BMF, the BM flush was loaded into the hollow core and capped with a disk of the mineralized matrix to confine the flush (*SI Appendix*, *SI Experimental Procedures* and Fig. S1). Synthetic matrices seeded with BMC or BMF were subcutaneously implanted into congenic mice to test for their ability to form bone tissue with a marrow compartment in a spatially confined manner. Fig. 1*A* summarizes the experimental procedures. Implantation of BMC and BMF constructs in GFP-positive mice revealed abundant donor CD45-positive hematopoietic cells (red) in the inner compartment of the tissue (Fig. 1*B*), suggesting the maintenance of donor hematopoietic cells by the engineered bone tissue. The gross appearance of the excised implants at 4 wk postimplantation suggests formation of hard tissue with observable vascular networks (*SI Appendix*, Fig. S5*A*). Three-dimensional microcomputed tomography (μCT) showed that implants (BMC- and BMF-laden matrices) that were initially undetectable before implantation (*SI Appendix*, Fig. S5*A*) had progressed to a hard tissue with calcification confined mostly within the outer compartment and with no significant hard tissue formation in the inner compartment for both BMC and BMF groups (*SI Appendix*, Fig. S5 *A* and *B* and Movies S1 and S2). Quantification of the μCT images for bone volume corroborated the above-mentioned observations (*SI Appendix*, Fig. S5*C*). Formation of hard tissues with dual compartments exhibiting differentially cellularized regions and abundance

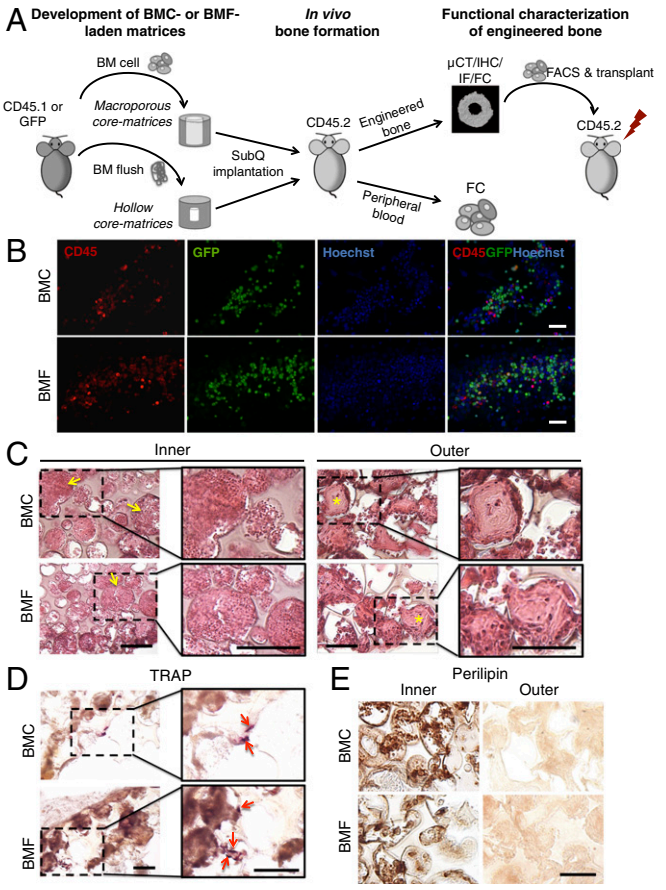

Fig. 1. Implanted BMC- and BMF-laden matrices matured in vivo into bone tissue harboring hematopoietic cells. (*A*) Schematic of experimental design. BMC- or BMF-laden matrices were implanted subcutaneously into mice and characterized for bone tissue formation, BM hematopoietic maintenance, donor chimerism, and hematopoietic reconstitution. (*B*) Immunofluorescent staining images of donor (red) and host (yellow in merged image) CD45-positive hematopoietic cells in BMC- and BMF-laden matrices 4 wk postimplantation in GFP mice. (Scale bar: 100 μm.) (*C*) H&E staining of inner and outer compartments of the engineered bone derived from BMC- or BMF-laden matrices after 4 wk of transplantation. Higher magnification images are also provided. The staining was performed on the outer and inner compartments of the engineered bone. Yellow arrows indicate hematopoietic-like cells. Yellow asterisks indicate woven bone-like tissue. Native murine bone with BM (*SI Appendix*, Fig. S5*B*) was used as a control. (Scale bar: 50 μm.) (*D*) Histochemical staining for tartrate-resistant acidic phosphatase (TRAP) in the outer compartment after 4 wk of implantation. Higher magnification images are also provided. Red arrows indicate TRAP-positive stain. (Scale bar: 200 μm.) (*E*) Immunohistochemical staining for perilipin, an adipocyte-specific marker, after 4 wk implantation of BMC- or BMF-laden matrices. (Scale bar: 50 μm.) Inner, inner compartment, Outer, outer compartment.

of extracellular matrix was confirmed by hematoxylin and eosin (H&E) staining. The histological analysis revealed a high cell density in the inner compartment for both the BMC and BMF groups, similar to the high cellularity found in native BM (Fig. 1*C* and *SI Appendix*, Fig. S5*D*). As evident from the H&E staining, the outer compartment of the implanted constructs exhibited woven bone-like structures (Fig. 1*C*). To investigate whether osteoclast-like cells are present in the engineered bone tissue, a tartrate-resistant acid phosphatase (TRAP) assay was carried out. Positive TRAP signals were observed in both the BMC and BMF groups in the outer calcified compartment (Fig. 1*D*). The sorted TRAP-positive cells were positive for cathepsin K gene expression as shown by cycle threshold value but undetectable in TRAP-negative cells (*SI Appendix*, Fig. S6*A*). Flow cytometric analyses of the outer calcified compartment showed that the majority of CD45/TRAP double-positive cells originated from donor cells whereas some were of host origin (*SI Appendix*, Fig. S6*B*). Although precursors of osteoclasts reside mostly in the BM (45, 46), these precursors are also detected in the circulation (47) and likely also contributed to the presence of host TRAP-positive cells in engineered bone. The coexistence of TRAP-positive osteoclast-like cells with osteoblasts implies potential remodeling of the engineered bone (48–50). Contrary to TRAP, immunohistochemical staining for perilipin, a marker of adipocytes, was found to be concentrated in the inner compartment of the engineered bone (Fig. 1*E*). This is consistent with native marrow because fat is a constituent of bone marrow, but absent in calcified tissues.

Immunohistochemical staining for osteocalcin, an osteoblast matricellular protein, showed higher intensity in the outer compartment compared with the inner compartment at 4 wk (*SI Appendix*, Fig. S7 *A–C*). The intensity of osteocalcin staining decreased as a function of time after 12 wk, which indicates the maturation of the neo-bone tissue (*SI Appendix*, Fig. S7 *D–F*). Osteopontin and bone sialoprotein gene expressions were also up-regulated in the outer compartment (*SI Appendix*, Fig. S8 *A* and *B*). Furthermore, the presence of collagen, a protein abundant in bone ECM, was also significantly higher in the outer compartment compared with the inner compartment as demonstrated by picrosirius red staining and the mean histogram intensity of the corresponding images (*SI Appendix*, Fig. S9 *A–C*). Because macroporous mineralized matrices are inherently osteoinductive (38, 42), the accumulated calcification and bone-specific ECM proteins within the mineralized outer compartment could have resulted from the differentiation of osteoprogenitor cells and the build-up of osteoblast-secreted ECM. We have previously shown that the macroporous mineralized materials can contribute to ectopic bone tissue formation through cells recruited from the recipient (38, 51). The vascularization of the engineered bone was characterized by immunofluorescent staining for CD31 (PECAM1), which shows the presence of vascular endothelial cells in both BMC and BMF groups (*SI Appendix*, Fig. S10*A*). Flow cytometric analyses of CD31-postive cells further reveal that a similar ratio of donor and host cells contributed to the endothelial cell population of the engineered bones (*SI Appendix*, Fig. 10*B*).

Taken together, the results from μCT and histology showed that both the BMC and BMF implants in vivo matured into dual-compartment structures with cellular and ECM characteristics similar to native bone tissues with a marrow compartment. Unlike prior studies that displayed random calcification at the site of implanted BM (17, 18, 21, 23), the dual-compartment structure with differential calcification facilitated spatially controlled bone tissue formation confined to the outer compartment with minimal calcification in the inner compartment. The engineered bone exhibiting a dual-compartment structure with an inner marrow compartment harbored by an outer shell of bone resembles the transverse plane of long bones.

Maintenance of Donor and Host Hematopoietic Cells in Engineered Bone. The maintenance of donor hematopoietic cells within the engineered bone was determined for different host environments including congenic, syngenic, and irradiated mice (*SI Appendix*, Fig. S11*A*). Analysis of the implanted BMC and BMF constructs at 1 d postimplantation showed that the donor cells in irradiated mice had less apoptosis and necrosis than those in nonirradiated congenic recipients (*SI Appendix*, Fig. S11 *B–E*). The donor hematopoietic cells were found in all engineered bone tissues with those in irradiated recipient mice harboring more donor cells over time than nonirradiated recipient mice (*SI Appendix*, Fig. S11 *F* and *G*). Donor hematopoietic cell numbers in irradiated recipients remained stable over 1–3 mo (*SI Appendix*, Fig. S11 *F* and *G*).

Immunofluorescent staining showed the presence of rare $CD150^+CD48^-$ hematopoietic cells within the engineered bone (both BMC and BMF groups) after 4 wk of implantation, suggesting the presence of hematopoietic stem and progenitor cells (HSPCs) (Fig. 2*A*) (52). As expected, engineered bones in irradiated congenic mice contained more LT-HSCs ($L^-S^+K^+CD150^+CD48^-CD34^-$), short-term HSCs (ST-HSCs; $L^-S^+K^+CD150^+CD48^-CD34^+$), multipotent progenitors (MPP; $L^-S^+K^+CD150^-CD48^-CD34^+$), common lymphoid progenitors (CLP; $L^-S^{low}K^{low}CD127^+CD34^+$), and common myeloid progenitors (CMP; $L^-S^-K^+CD16/32^-CD34^+$) than did bones in nonirradiated mice (Fig. 2 *B–F* and *SI Appendix*, Figs. S12 and S13*A*). Mature cells of donor origin such as T ($CD3^+$), B ($B220^+$), and myeloid cells ($CD11b^+$) were also found within the engineered bone of nonirradiated congenic mice (*SI Appendix*, Fig. S13*B*). Similar findings were also observed with the nonirradiated syngenic recipients (*SI Appendix*, Fig. S14 *A–C*).

The presence of vasculature suggests that cells may migrate between the engineered bone and the host circulation. In addition to donor cells, host hematopoietic cells were also found in the implanted BMC and BMF groups in congenic and syngenic mice (nonirradiated). Similar numbers of host cells, LT-HSCs, ST-HSCs, MPPs, CMPs, and CLPs and frequencies of HSPCs were found in the BMC and BMF groups after 4 wk irrespective of the host environment (syngenic vs. congenic). The number of host cells within the implants increased over time in both congenic (*SI Appendix*, Fig. S13 *C–F*) and syngenic recipients (*SI Appendix*, Fig. S14 *D–F*). Furthermore, host mature T, B, and myeloid cell populations were also found within the engineered bone tissues (both BMC and BMF groups) (*SI Appendix*, Fig. S13*F*).

The recruitment of host cells could either be elicited by the presence of BM cells present in the engineered bone that may secrete abundant chemokines and cytokines (53) or be the result of an immune response to the foreign implant (54–57). We believe that the engineered BM is not merely an attractor of immune cells but one that offers a hematopoietic environment as many key populations of the host hematopoietic cell lineages were found within the engineered bone. Furthermore, hematopoietic cells were maintained over 3 mo in engineered bone, which is a considerably longer time than migration and the presence of lymphocytes due to inflammatory responses. We also investigated the colony-forming ability of the hematopoietic cells derived from the BMC and BMF constructs 4 wk postimplantation. The in vitro colony-forming assay showed that the cells derived from the BMC and BMF groups were able to develop into colony-forming units including CFU-GEMM, CFU-GM, and BFU-E (*SI Appendix*, Fig. S15 *A–C*).

Because the dimensions of the inner compartment of the BMC and BMF groups were different, we determined the effect of the size of the inner compartment on the hematopoietic maintenance. To this end, we assembled BMC constructs with an inner dimension similar to that of BMF constructs, which we denoted BMC-S (*SI Appendix*, Fig. S16*A*). Comparing the ability of BMC-S to support hematopoietic cells with that of BMC

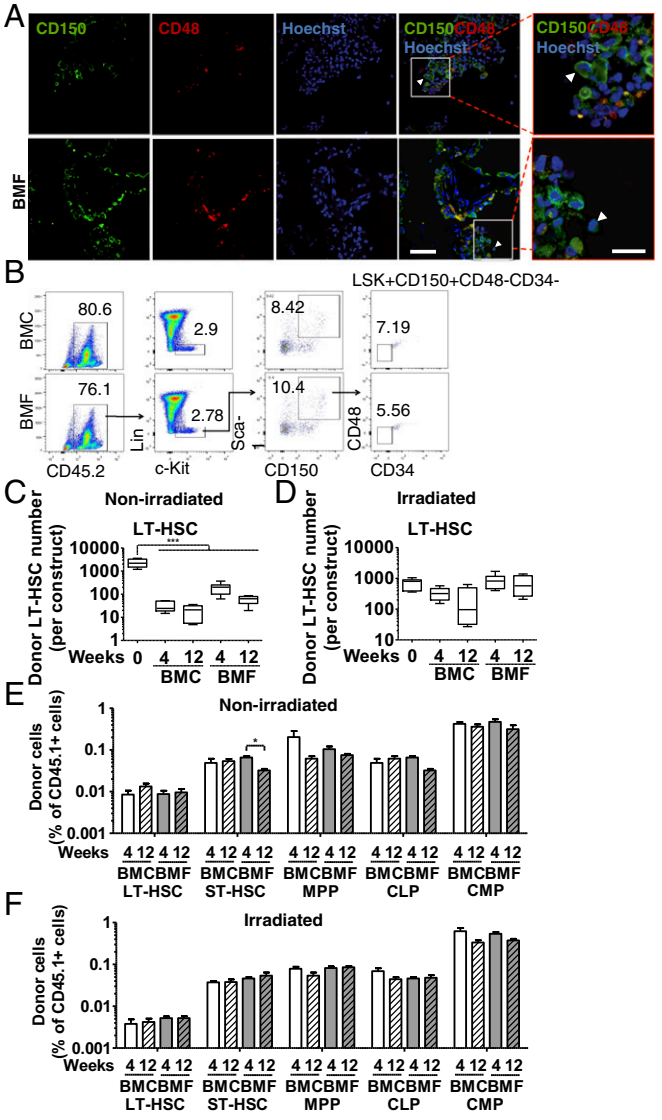

Fig. 2. Presence of hematopoietic stem and progenitor cells in engineered bone. (*A*) Immunofluorescent staining for $CD150^{+}CD48^{-}$ cells representing the HSPC population (white arrowhead). CD150-positive cells (green), CD48-positive cells (red), and Hoechst (blue; nucleus). (Scale bar: 500 μm; high magnification scale bar: 200 μm.) (*B*) Flow cytometric analysis of LT-HSCs represented by the LSK+CD150+CD48−CD34− fraction from BMC and BMF matrices. (*C*) Absolute number of donor LT-HSCs per implant in nonirradiated congenic recipient mice. (*D*) Absolute number of donor LT-HSC per implant in lethally irradiated congenic recipient mice. (*E*) Percentage of donor hematopoietic stem and progenitor cell numbers per implant in nonirradiated congenic recipients. (*F*) Percentage of donor hematopoietic stem and progenitor cell numbers per implant in lethally irradiated congenic recipients. Data are presented as mean ± SE obtained from six engineered bones ($n = 6$). One-way ANOVA with Tukey post hoc test. $^{*}P < 0.05$. $^{***}P < 0.001$.

groups showed that the total donor hematopoietic cell and LT-HSC numbers were not significantly different between the two implants after 4 wk of implantation (*SI Appendix*, Fig. S16 *B* and *C*).

Donor Chimerism and Hematopoietic Reconstitution. Because the engineered bones are vascularized and maintain hematopoietic lineages in vivo, we looked into whether the hematopoietic cells of the BMC and BMF constructs were functional by investigating the presence of donor cells in circulation. After 4 wk and 24 wk of BMC or BMF construct implantation, peripheral blood was harvested, and the fraction of donor and host hematopoietic cells was analyzed and compared against that of tail-vein injection and/or kidney capsule implantation involving similar cell numbers (Fig. 3*A*). Donor cell chimerism was detected in all animals bearing the engineered bones with 3.91 ± 0.69% and 4.11 ± 0.67% for BMC and BMF groups, respectively, compared with 0.66 ± 0.52% for the tail-vein–injected group and 4.58 ± 0.90% for the kidney capsule implantation group after 4 wk. Similar levels of donor cell chimerism were observed 24 wk post-implantation of BMC and BMF groups (Fig. 3*B*). These results showed that the engineered bone supports long-term maintenance of the donor marrow cells without recipient conditioning. The number of HSCs within the engineered bone tissues would be a key factor in determining their hematopoietic function, as more cell survival would lead to higher donor cell number and frequency of donor chimerism. Prior studies have shown a positive correlation between the number of transplanted HSPCs or BM cells to the engraftment efficiency in nonmyeloablated recipients (58–61). The modular dual-compartment scaffold offers an enabling screening platform to identify optimal factors (cellular and extracellular components) that support hematopoiesis.

To further validate the hematopoietic function of the engineered bone, the HSPC mobilization agent chemokine (C-X-C motif) receptor 4 (CXCR4) antagonist, AMD 3100, was administered into mice implanted with the BMC- and BMF-laden matrices. The results were compared against mice receiving

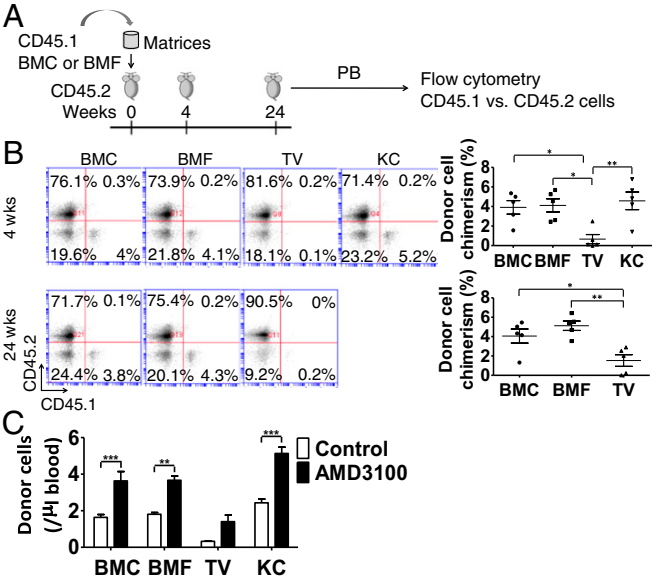

Fig. 3. Engineered bone supports mobilization of donor cells into circulation. (*A*) Schematic of experimental procedures. CD45.1-positive BMC- or BMF-loaded matrices were implanted subcutaneously in CD45.2 mice. After 4 wk and 24 wk, peripheral blood (PB) was harvested and analyzed for the presence of donor (CD45.1) and host (CD45.2) cells. (*B*) Flow cytometric analysis of the percentage donor cell chimerism after 4 wk and 24 wk of BMC- or BMF-laden matrices, compared against tail-vein–injected (TV) and/or kidney-capsule–implanted (KC) groups. Data are presented as mean ± SEs ($n = 6$). (*C*) Flow cytometric analysis of donor cells in peripheral blood of recipient mice bearing BMC- and BMF-laden matrices with or without AMD 3100 administration. After 4 wk of implantation, the HSC mobilization agent AMD 3100 was administered for 1 h, and peripheral blood was harvested and analyzed for the presence of donor (CD45.1) cells. The values were compared against TV and KC groups. Data are presented as mean ± SEs obtained from PB of five mice ($n = 5$). One-way ANOVA with Tukey post hoc test. $^{*}P < 0.05$. $^{**}P < 0.01$. $^{***}P < 0.001$.

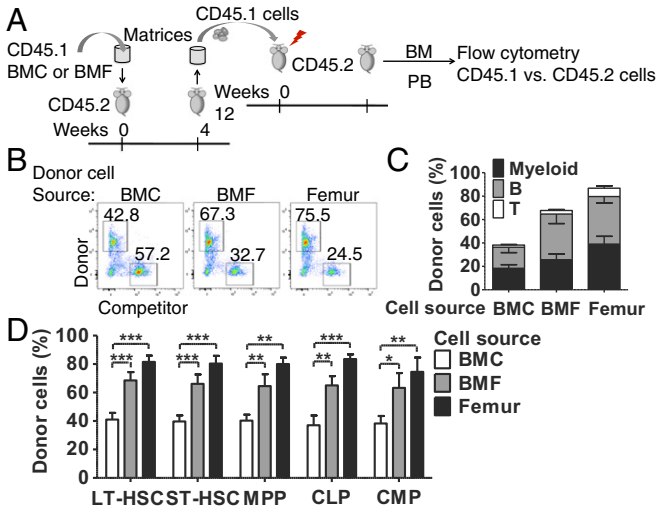

Fig. 4. Hematopoietic cells from engineered bone supports hematopoietic reconstitution in secondary mice. (*A*) Schematic of experimental procedures. CD45.1-positive BMC or BMF were seeded into matrices and implanted subcutaneously in CD45.2 mice. After 4 wk, 4×10^5 donor CD45.1 cells were sorted by FACS from engineered bone tissue and injected along with 2.5×10^5 support CD45.2 cells into lethally irradiated CD45.2 mice. Donor hematopoietic reconstitution was analyzed 3 mo after transplantation. (*B*) Percentage of donor CD45.1-positive hematopoietic cells was analyzed in PB of recipient mice injected with cells isolated from BMC and BMF. (*C*) Percentage of donor CD45.1-positive myeloid, T, and B cells in PB of recipient mice injected with cells isolated from the engineered bone tissues (BMC and BMF groups). (*D*) Percentage of donor CD45.1-positive hematopoietic stem and progenitor cells in BM of recipient mice injected with cells isolated from the engineered bone tissues. Donor cells from the femur serve as control. One-way ANOVA with Tukey post hoc test. $*P < 0.05$. $**P < 0.01$. $***P < 0.001$.

similar number of cells through tail-vein injection or kidney capsule implantation. Upon administration of AMD 3100, donor cells from both BMC and BMF groups were mobilized into the circulation resulting in a significantly higher number of cells in the peripheral blood than in the basal state (Fig. 3*C*). The donor cells in circulation were significantly higher than those of the i.v.-injected group but similar to kidney capsule implantation. This suggests that the functional responsiveness of donor cells, including HSPCs, is mobilized from the engineered bone into the circulation (62, 63). Flow cytometric analysis did not detect any donor cells within the host BM, suggesting that the presence of donor cells in the circulation directly originated from the engineered bone and not through the host BM.

The function of donor hematopoietic cells from engineered bone was further examined by transplanting donor CD45.1 cells along with CD45.2 support (competitor) cells into lethally irradiated CD45.2 mice (Fig. 4*A*). Among the BMF and BMC groups, donor myeloid and B and T cells from the BMF groups were found at a higher percentage in the peripheral blood of the recipient CD45.2 mice than those from the BMC group (Fig. 4 *B* and *C*). Various lineages of donor HSPCs were also found in the recipient BM, wherein BMF-derived cells exhibited a higher reconstitution of HSPCs in the host compared with the BMC-derived cells (Fig. 4*D*). This could be due to the BM ECM present in BMF groups, which is lacking in the BMC group.

Together, the results showed that the engineered bone with a marrow compartment not only attained a higher donor cell chimerism compared with i.v. injection, but also responded to the HSPC mobilization drug AMD 3100. These attributes could have tremendous implications in translational medicine and suggest that the engineered bone maintains a functional HSC niche with a selective advantage of donor cell survival over i.v. injection. Such easy-to-use and cost-effective tissue-engineered bone could potentially be used as HSPC or BM surrogates of allogeneic donor cells as an alternative method for cell transplantation to treat various non-malignant hematopoietic diseases (64). This approach could require fewer cell numbers than conventional i.v. injection and prevent the need for recipient conditioning while achieving higher mixed chimerism in recipients of hematopoietic cell transplantation. Moreover, the engineered bone could be applied as a technological platform to understand how individual BM cell populations or ECM affect hematopoietic functions within the marrow compartment during hematopoietic development, homeostasis, aging, and disease.

Experimental Procedures

Detailed methods are described in *SI Appendix, SI Experimental Procedures*. All experiments were conducted with a sample size of $n \geq 3$ and were also independently repeated at least twice.

Synthesis of PEGDA-*co*-A6ACA Hydrogels and Macroporous Hydrogels. Macroporous poly(ethylene glycol)-diacrylate (PEGDA) ($M_n = 3.4$ kDa)-*co*-*N*-acryloyl 6-aminocaproic acid (A6ACA) hydrogels were synthesized as previously described (38).

Biomineralization of Hydrogels and Macroporous Hydrogels. Biomineralization of the PEGDA-*co*-A6ACA macroporous hydrogels was carried out as described elsewhere (38).

BMHarvest and ex Vivo Seeding into Matrices. C57BL/6J (CD45.2), B6.SJL-Ptprc^a Pepc^b/BoyJ (CD45.1), and C57BL/6-Tg(UBC-GFP)30Scha/J (Jackson Laboratory) mice were bred in the specific pathogen-free area of the institutional animal facility and maintained in a clean region of the facility during the experiments. Two- to three-month-old mice were used for all of the experiments. All experiments were approved by the Institutional Animal Care and Use Committee of the University of California, San Diego, and were performed in accordance with national and international guidelines for laboratory animal care. BMCs were prepared by repeated pipetting of the BM flush in growth medium to disrupt the cells and ECM. Cells were collected by passing through a cell strainer (40 μm) and centrifuged at $300 \times g$. On the other hand, the BMFs were prepared without disturbing the whole BM and left intact once it was flushed out.

ACKNOWLEDGMENTS. The hMSCs used in this study were provided by Texas A&M University (NIH Grant P40RR017447). This work was supported by the NIH (Grant 1 R01 AR063184-01A1) and by the California Institute of Regenerative Medicine (Grant RT2-01889).

1. Ikehara S (1998) Bone marrow transplantation for autoimmune diseases. *Acta Haematol* 99:116–132.
2. Kanakry CG, Fuchs EJ, Luznik L (2016) Modern approaches to HLA-haploidentical blood or marrow transplantation. *Nat Rev Clin Oncol* 13:132.
3. Sykes M, Nikolic B (2005) Treatment of severe autoimmune disease by stem-cell transplantation. *Nature* 435:620–627.
4. Dvorak CC, Cowan MJ (2008) Hematopoietic stem cell transplantation for primary immunodeficiency disease. *Bone Marrow Transplant* 41:119–126.
5. Peters C, Steward CG; National Marrow Donor Program; International Bone Marrow Transplant Registry; Working Party on Inborn Errors, European Bone Marrow Transplant Group (2003) Hematopoietic cell transplantation for inherited metabolic diseases: An overview of outcomes and practice guidelines. *Bone Marrow Transplant* 31:229–239.
6. Locatelli F, et al.; Eurocord and European Blood and Marrow Transplantation (EBMT) group (2013) Outcome of patients with hemoglobinopathies given either cord blood or bone marrow transplantation from an HLA-identical sibling. *Blood* 122:1072–1078.
7. McCracken MN, et al. (2013) Long-term in vivo monitoring of mouse and human hematopoietic stem cell engraftment with a human positron emission tomography reporter gene. *Proc Natl Acad Sci USA* 110:1857–1862.
8. Marquez-Curtis LA, Turner AR, Sridharan S, Ratajczak MZ, Janowska-Wieczorek A (2011) The ins and outs of hematopoietic stem cells: Studies to improve transplantation outcomes. *Stem Cell Rev* 7:590–607.
9. Horan J, et al. (2012) Evaluation of HLA matching in unrelated hematopoietic stem cell transplantation for nonmalignant disorders. *Blood* 120:2918–2924.
10. Klein OR, et al. (2016) Alternative-donor hematopoietic stem cell transplantation with post-transplantation cyclophosphamide for nonmalignant disorders. *Biol Blood Marrow Transplant* 22:895–901.
11. Sullivan KM, Parkman R, Walters MC (2000) Bone marrow transplantation for nonmalignant disease. *Hematology (Am Soc Hematol Educ Program)* 2000:319–338.

12. Gyurkocza B, Sandmaier BM (2014) Conditioning regimens for hematopoietic cell transplantation: one size does not fit all. *Blood* 124:344–353.
13. Schofield R (1978) The relationship between the spleen colony-forming cell and the haemopoietic stem cell. *Blood Cells* 4:7–25.
14. Baker KS, et al. (2007) Diabetes, hypertension, and cardiovascular events in survivors of hematopoietic cell transplantation: A report from the bone marrow transplantation survivor study. *Blood* 109:1765–1772.
15. Borgmann-Staudt A, et al. (2012) Fertility after allogeneic haematopoietic stem cell transplantation in childhood and adolescence. *Bone Marrow Transplant* 47:271–276.
16. Sakiyama M, et al.; Tokyo SCT Consortium (2004) Regimen-related toxicity following reduced-intensity stem-cell transplantation (RIST): Comparison between Seattle criteria and National Cancer Center Common Toxicity Criteria (NCI-CTC) version 2.0. *Bone Marrow Transplant* 34:787–794.
17. Friedenstein AJ, Petrakova KV, Kurolesova AI, Frolova GP (1968) Heterotopic of bone marrow. Analysis of precursor cells for osteogenic and hematopoietic tissues. *Transplantation* 6:230–247.
18. Amsel S, Dell ES (1971) Bone marrow repopulation of subcutaneously grafted mouse femurs. *Proc Soc Exp Biol Med* 138:550–552.
19. Chan CK, et al. (2009) Endochondral ossification is required for haematopoietic stem-cell niche formation. *Nature* 457:490–494.
20. Torisawa YS, et al. (2014) Bone marrow-on-a-chip replicates hematopoietic niche physiology in vitro. *Nat Methods* 11:663–669.
21. Krupnick AS, Shaaban A, Radu A, Flake AW (2002) Bone marrow tissue engineering. *Tissue Eng* 8:145–155.
22. Scotti C, et al. (2013) Engineering of a functional bone organ through endochondral ossification. *Proc Natl Acad Sci USA* 110:3997–4002.
23. Chen Y, et al. (2012) Human extramedullary bone marrow in mice: A novel in vivo model of genetically controlled hematopoietic microenvironment. *Blood* 119: 4971–4980.
24. Fujita A, et al. (2010) Hematopoiesis in regenerated bone marrow within hydroxyapatite scaffold. *Pediatr Res* 68:35–40.
25. Reinisch A, et al. (2016) A humanized bone marrow ossicle xenotransplantation model enables improved engraftment of healthy and leukemic human hematopoietic cells. *Nat Med* 22:812–821.
26. Ventura Ferreira MS, et al. (2016) An engineered multicomponent bone marrow niche for the recapitulation of hematopoiesis at ectopic transplantation sites. *J Hematol Oncol* 9:4.
27. Lee J, et al. (2012) Implantable microenvironments to attract hematopoietic stem/cancer cells. *Proc Natl Acad Sci USA* 109:19638–19643.
28. Sacchetti B, et al. (2007) Self-renewing osteoprogenitors in bone marrow sinusoids can organize a hematopoietic microenvironment. *Cell* 131:324–336.
29. Méndez-Ferrer S, et al. (2010) Mesenchymal and haematopoietic stem cells form a unique bone marrow niche. *Nature* 466:829–834.
30. Park D, et al. (2012) Endogenous bone marrow MSCs are dynamic, fate-restricted participants in bone maintenance and regeneration. *Cell Stem Cell* 10:259–272.
31. Greenbaum A, et al. (2013) CXCL12 in early mesenchymal progenitors is required for haematopoietic stem-cell maintenance. *Nature* 495:227–230.
32. Zhang J, et al. (2003) Identification of the haematopoietic stem cell niche and control of the niche size. *Nature* 425:836–841.
33. Calvi LM, et al. (2003) Osteoblastic cells regulate the haematopoietic stem cell niche. *Nature* 425:841–846.
34. Naveiras O, et al. (2009) Bone-marrow adipocytes as negative regulators of the haematopoietic microenvironment. *Nature* 460:259–263.
35. Kobayashi H, et al. (2010) Angiocrine factors from Akt-activated endothelial cells balance self-renewal and differentiation of haematopoietic stem cells. *Nat Cell Biol* 12:1046–1056.
36. Hooper AT, et al. (2009) Engraftment and reconstitution of hematopoiesis is dependent on VEGFR2-mediated regeneration of sinusoidal endothelial cells. *Cell Stem Cell* 4:263–274.
37. Domingues MJ, Cao H, Heazlewood SY, Cao B, Nilsson SK (January 23, 2017) Niche Extracellular Matrix Components and their influence on HSC. *J Cell Biochem*, 10.1002/jcb.25905.
38. Shih YR, et al. (2015) Synthetic bone mimetic matrix-mediated in situ bone tissue formation through host cell recruitment. *Acta Biomater* 19:1–9.
39. Zhang CAA, Liao L, Varghese S (2009) A novel single precursor-based biodegradable hydrogel with enhanced mechanical properties. *Soft Matter* 5:3831–3834.
40. Phadke A, Zhang C, Hwang Y, Vecchio K, Varghese S (2010) Templated mineralization of synthetic hydrogels for bone-like composite materials: Role of matrix hydrophobicity. *Biomacromolecules* 11:2060–2068.
41. Ayala R, et al. (2011) Engineering the cell-material interface for controlling stem cell adhesion, migration, and differentiation. *Biomaterials* 32:3700–3711.
42. Shih YR, et al. (2014) Calcium phosphate-bearing matrices induce osteogenic differentiation of stem cells through adenosine signaling. *Proc Natl Acad Sci USA* 111: 990–995.
43. Kang H, et al. (2014) Biomineralized matrix-assisted osteogenic differentiation of human embryonic stem cells. *J Mater Chem B Mater Biol Med* 2:5676–5688.
44. Kang H, Shih YR, Varghese S (2015) Biomineralized matrices dominate soluble cues to direct osteogenic differentiation of human mesenchymal stem cells through adenosine signaling. *Biomacromolecules* 16:1050–1061.
45. Xiao Y, et al. (2013) Osteoclast precursors in murine bone marrow express CD27 and are impeded in osteoclast development by CD70 on activated immune cells. *Proc Natl Acad Sci USA* 110:12385–12390.
46. Jacquin C, Gran DE, Lee SK, Lorenzo JA, Aguila HL (2006) Identification of multiple osteoclast precursor populations in murine bone marrow. *J Bone Miner Res* 21:67–77.
47. Kotani M, et al. (2013) Systemic circulation and bone recruitment of osteoclast precursors tracked by using fluorescent imaging techniques. *J Immunol* 190:605–612.
48. Helmrich U, et al. (2013) Osteogenic graft vascularization and bone resorption by VEGF-expressing human mesenchymal progenitors. *Biomaterials* 34:5025–5035.
49. Scotti C, Hirschmann MT, Antinolfi P, Martin I, Peretti GM (2013) Meniscus repair and regeneration: Review on current methods and research potential. *Eur Cell Mater* 26: 150–170.
50. Song G, et al. (2013) The homing of bone marrow MSCs to non-osseous sites for ectopic bone formation induced by osteoinductive calcium phosphate. *Biomaterials* 34: 2167–2176.
51. Phadke A, et al. (2013) Effect of scaffold microarchitecture on osteogenic differentiation of human mesenchymal stem cells. *Eur Cell Mater* 25:114–128; discussion 128–129.
52. Yilmaz OH, Kiel MJ, Morrison SJ (2006) SLAM family markers are conserved among hematopoietic stem cells from old and reconstituted mice and markedly increase their purity. *Blood* 107:924–930.
53. Cao Y, et al. (2010) The cytokine/chemokine pattern in the bone marrow environment of multiple myeloma patients. *Exp Hematol* 38:860–867.
54. Anderson JM, Rodriguez A, Chang DT (2008) Foreign body reaction to biomaterials. *Semin Immunol* 20:86–100.
55. Higgins DM, et al. (2009) Localized immunosuppressive environment in the foreign body response to implanted biomaterials. *Am J Pathol* 175:161–170.
56. Veiseh O, et al. (2015) Size- and shape-dependent foreign body immune response to materials implanted in rodents and non-human primates. *Nat Mater* 14:643–651.
57. Nair A, et al. (2011) Biomaterial implants mediate autologous stem cell recruitment in mice. *Acta Biomater* 7:3887–3895.
58. Christopherson KW, II, Hangoc G, Mantel CR, Broxmeyer HE (2004) Modulation of hematopoietic stem cell homing and engraftment by CD26. *Science* 305:1000–1003.
59. Stewart FM, Crittenden RB, Lowry PA, Pearson-White S, Quesenberry PJ (1993) Long-term engraftment of normal and post-5-fluorouracil murine marrow into normal nonmyeloablated mice. *Blood* 81:2566–2571.
60. Sykes M, Szot GL, Swenson K, Pearson DA, Wekerle T (1998) Separate regulation of peripheral hematopoietic and thymic engraftment. *Exp Hematol* 26:457–465.
61. Nilsson SK, Dooner MS, Tiarks CY, Weier HU, Quesenberry PJ (1997) Potential and distribution of transplanted hematopoietic stem cells in a nonablated mouse model. *Blood* 89:4013–4020.
62. Broxmeyer HE, et al. (2005) Rapid mobilization of murine and human hematopoietic stem and progenitor cells with AMD3100, a CXCR4 antagonist. *J Exp Med* 201: 1307–1318.
63. Smith-Berdan S, et al. (2011) Robo4 cooperates with CXCR4 to specify hematopoietic stem cell localization to bone marrow niches. *Cell Stem Cell* 8:72–83.
64. Shenoy S, Boelens JJ (2015) Advances in unrelated and alternative donor hematopoietic cell transplantation for nonmalignant disorders. *Curr Opin Pediatr* 27:9–17.